

RESEARCH ARTICLE | *Building Neural Circuits: Wiring and Experience*

Wakefulness suppresses retinal wave-related neural activity in visual cortex

Didhiti Mukherjee,^{1,4} Alex J. Yonk,¹  Greta Sokoloff,^{1,4} and Mark S. Blumberg^{1,2,3,4}

¹Department of Psychological and Brain Sciences, University of Iowa, Iowa City, Iowa; ²Interdisciplinary Graduate Program in Neuroscience, University of Iowa, Iowa City, Iowa; ³Department of Biology, University of Iowa, Iowa City, Iowa; and ⁴DeLTA Center, University of Iowa, Iowa City, Iowa

Submitted 7 April 2017; accepted in final form 8 June 2017

Mukherjee D, Yonk AJ, Sokoloff G, Blumberg MS. Wakefulness suppresses retinal wave-related neural activity in visual cortex. *J Neurophysiol* 118: 1190–1197, 2017. First published June 14, 2017; doi:10.1152/jn.00264.2017.—In the developing visual system before eye opening, spontaneous retinal waves trigger bursts of neural activity in downstream structures, including visual cortex. At the same ages when retinal waves provide the predominant input to the visual system, sleep is the predominant behavioral state. However, the interactions between behavioral state and retinal wave-driven activity have never been explicitly examined. Here we characterized unit activity in visual cortex during spontaneous sleep-wake cycles in 9- and 12-day-old rats. At both ages, cortical activity occurred in discrete rhythmic bursts, ~30–60 s apart, mirroring the timing of retinal waves. Interestingly, when pups spontaneously woke up and moved their limbs in the midst of a cortical burst, the activity was suppressed. Finally, experimentally evoked arousals also suppressed intraburst cortical activity. All together, these results indicate that active wake interferes with the activation of the developing visual cortex by retinal waves. They also suggest that sleep-wake processes can modulate visual cortical plasticity at earlier ages than has been previously considered.

NEW & NOTEWORTHY By recording in visual cortex in unanesthetized infant rats, we show that neural activity attributable to retinal waves is specifically suppressed when pups spontaneously awaken or are experimentally aroused. These findings suggest that the relatively abundant sleep of early development plays a permissive functional role for the visual system. It follows, then, that biological or environmental factors that disrupt sleep may interfere with the development of these neural networks.

visual cortex; development; spontaneous activity; retinal wave; sleep; wake; neural plasticity

SPONTANEOUS ACTIVITY is a signature feature of the developing nervous system (Blankenship and Feller 2010; Blumberg et al. 2013) that facilitates such fundamental neurodevelopmental processes as migration, synaptogenesis, differentiation, and topographic organization (Katz and Shatz 1996; Kilb et al. 2011; Marder and Rehm 2005). In the visual system, spontaneous activity occurs in the form of retinal waves (Wong 1999). The neural activity that arises from retinal waves cascades through the visual system, including the lateral geniculate nucleus (LGN) and visual cortex (Ackman et al. 2012; Hanganu et al. 2006; Mooney et al. 1996), and is thought to

facilitate eye-specific segregation of retinofugal projections (Butts et al. 2007), refinement of receptive field characteristics (Huberman et al. 2008), and the formation of retinotopic maps (Ackman et al. 2012; Wong 1999).

When retinal waves are the predominant form of activity in the visual system, sleep is the predominant behavioral state (Gramsbergen et al. 1970; Jouvet-Mounier et al. 1970). Nonetheless, previous studies of visual cortical activity have not explicitly assessed whether retinal wave-related neural activity is modulated by behavioral state (but see Colonnese et al. 2010; Mirmiran and Corner 1982). And although wake movements in infant mice have been associated with the suppression of spontaneously generated calcium waves in several nonvisual cortical areas (Adelsberger et al. 2005), it has never been demonstrated that wake movements suppress retinal wave-driven activity in visual cortex.

To address this issue, we used extracellular neurophysiology to characterize the spontaneous activity of visual cortical neurons in infant rats as they cycled normally between sleep and wake. We found bursts of rhythmic unit activity that occurred approximately every 30–60 s—indicative of retinal wave activity—in the visual cortex at both ages. Interestingly, when pups woke up and moved their limbs, we observed a rapid suppression of cortical activity. Moreover, when these awakenings occurred during a retinal wave-related burst—and regardless of whether the awakening was spontaneous or evoked by the experimenter—the associated burst of cortical activity was interrupted. Together, these findings demonstrate that behavioral state modulates neural activity in the developing visual system and suggest a role for sleep in visual system plasticity at earlier ages than has previously been considered (Frank et al. 2001; Shaffery et al. 2002).

METHODS

All experiments were carried out in accordance with the National Institutes of Health (NIH) *Guide for the Care and Use of Laboratory Animals* (NIH Pub. No. 80-23). The experiments were also approved by the Institutional Animal Care and Use Committee (IACUC) of the University of Iowa.

Subjects. Male and female Sprague-Dawley Norway rats (*Rattus norvegicus*) at postnatal days (P)8–9 (hereafter P9; $n = 11$) and P11–12 (hereafter P12; $n = 20$) from 31 litters were used. All litters were culled to eight pups by P3. Mothers with their litters were housed and raised in standard laboratory cages (48 × 20 × 26 cm). Food and water were provided ad libitum. The animals were maintained on a

Address for reprint requests and other correspondence: M. S. Blumberg, Dept. of Psychological and Brain Sciences, University of Iowa, Iowa City, IA 52242 (e-mail: mark-blumberg@uiowa.edu).

12:12-h light-dark cycle with lights on at 0700. Littermates were never assigned to the same experimental group.

Surgery. A complete description of the head-fix method has been published (Blumberg et al. 2015). Briefly, under isoflurane (3–5%) anesthesia, stainless steel bipolar hook electrodes (50- μ m diameter; California Fine Wire, Grover Beach, CA) were inserted into the nuchal, forelimb, and hindlimb muscles for electromyography (EMG) and secured with collodion; a ground wire was secured transdermally on the back. A custom-built head-fix device was secured to the exposed skull with cyanoacrylate adhesive. Bupivacaine (0.25%) was applied topically to the site of incision as a local anesthetic; in addition, midway through the study (as a result of a change in IACUC protocol), pups were also injected subcutaneously with the analgesic agent carprofen (0.005 mg/g). The pup was then lightly wrapped in gauze and allowed to recover in a humidified, temperature-controlled (35–36°C) incubator for at least 1 h. After recovery, the pup was briefly reanesthetized with isoflurane (2–3%) and secured in a stereotaxic apparatus (David Kopf Instruments, Tujunga, CA). A hole was drilled in the skull over visual cortex for later insertion of the electrode (coordinates with respect to lambda: anteroposterior = 0–0.5 mm; mediolateral = 1.5–3.5 mm). Two additional holes allowed for insertion of the ground wire and a thermocouple (Omega Engineering, Stamford, CT) for measuring brain temperature. The animal was then transferred to the electrophysiology rig and prepared for recording.

Electrophysiology. The head-fix device was secured to the stereotaxic apparatus, and the pup was positioned with its body prone on a narrow platform and limbs dangling freely on both sides. Care was taken to regulate air temperature and humidity, and the pup's brain temperature was maintained at 36–37°C. Adequate time (1–2 h) was allowed for the pup to acclimate to the recording environment, and testing began only when it was cycling normally between sleep and wake. Pups rarely exhibited abnormal behavior or any signs of discomfort or distress; when they did, the experiment was terminated.

The bipolar EMG electrodes were connected to a differential amplifier (A-M Systems, Carlsborg, WA; amplification: 10,000 \times ; filter setting: 300–5,000 Hz). A ground wire (Ag/AgCl, 0.25-mm diameter; Medwire, Mt. Vernon, NY) was inserted into the parietal cortex contralateral to the recording site, and a thermocouple was inserted into the parietal cortex ipsilateral to the recording site. Neurophysiological recordings were performed with a 16-channel silicon electrode (NeuroNexus, Ann Arbor, MI) connected to a data acquisition system (Tucker-Davis Technologies, Alachua, FL) that amplified (10,000 \times) and filtered (500–5,000 Hz band pass) the neural signals. A digital interface and Spike2 software (Cambridge Electronic Design, Cambridge, UK) were used to acquire EMG and neurophysiological signals at 1 kHz and at least 12.5 kHz, respectively.

A micromanipulator (FHC, Bowdoinham, ME) was used to lower the electrode into visual cortex until action potentials were detected. Recording began at least 10 min after multiunit activity (MUA) was detected. Before insertion, the electrode was dipped in fluorescent 1,1'-diiododecyl-3,3,3',3'-tetramethylindocarbocyanine perchlorate (DiI) (Life Technologies, Grand Island, NY) for later identification of the recording site.

Procedure. With the pup cycling between sleep and wake and while continuously recording MUA and EMG activity, we first delivered 20 brief flashes of green LED light (Nite Ize, Boulder, CO) to each eye, with flashes spaced at least 5 s apart (Colonnese et al. 2010). Next, recording of MUA and EMG activity continued for 30 min as the pup cycled freely between sleep and wake. The experimenter, blind to the electrophysiological record, scored the pup's sleep and wake behaviors as described previously (Karlsson et al. 2005).

A total of 9 pups at P9 (yielding 22 units) and 12 pups at P12 (yielding 24 units) were used in this experiment. In the P12 subjects only, after the first 30-min recording period was complete we performed intraocular injections of tetrodotoxin citrate (TTX; dissolved

in 0.9% saline; Sigma-Aldrich, St. Louis, MO), as described previously (Hanganu et al. 2006). Before injection, bupivacaine (0.25%) was applied topically to the eyelid as a local anesthetic. With a 27-gauge needle attached to a microsyringe pump (Stoelting, Wood Dale, IL), 1 μ l of TTX (20 μ M) was injected into each eye at 0.5 μ l/min. After 20–30 min, spontaneous activity during sleep and wake was again recorded for 30 min. In 3 of 12 pups a total of five units were lost, and so data from these units were not analyzed further. Post-TTX injection data were analyzed in the remaining 19 units from nine pups.

Finally, an additional six P12 subjects from six different litters were prepared for recording as described above. Two experimenters were needed to conduct this experiment, one to monitor the electrophysiological record and the second to stimulate the pup. As the pup cycled between sleep and wake, when the first experimenter identified the onset of a cortical burst the second experimenter was quickly instructed to either stimulate the pup (Stim trials) or do nothing (No Stim trials). During the Stim trials, the second experimenter stimulated the pup's forelimbs or hindlimbs with a cotton-tipped applicator. At least 25 Stim and No Stim trials were performed for each pup with a randomized procedure. The first experimenter noted each trial with a key press synchronized with the electrophysiological record.

At the end of all recording sessions, pups were anesthetized with pentobarbital sodium (1.5 mg/g ip) or ketamine-xylazine (0.02 mg/g ip) and perfused transcardially with phosphate-buffered saline and 4% formaldehyde.

Retrograde tracing. An additional four P9 and P12 pups, two at each age, were used for anatomical tracing. Each pup was anesthetized with 2–5% isoflurane and secured in a stereotaxic apparatus. A 0.5- μ l syringe was lowered stereotaxically into the visual cortex, and 0.02 μ l of 2% wheat germ agglutinin (WGA) conjugated to Alexa Fluor 555 (WGA-555) (Invitrogen Life Technologies, Carlsbad, CA) was injected over 1 min. After a 15-min postinfusion period, the microsyringe was withdrawn and the incision was closed with Vet-bond (3M, Maplewood, MN). The pup was returned to its home cage and perfused 24 h later as described above.

Histology. Brains were sectioned coronally at 80 μ m with a freezing microtome (Leica Microsystems, Buffalo Grove, IL). Recording sites were determined by examining DiI tracks before and after staining with cresyl violet with a fluorescent microscope (Leica Microsystems). For retrograde tracing with WGA-555, brains were sectioned coronally at 50 μ m and alternating sections were stained with cresyl violet.

Spike sorting. As described previously (Sokoloff et al. 2015a, 2015b), action potentials (signal-to-noise ratio \geq 2:1) were sorted from MUA records with the template-matching algorithm in Spike2 with a 1-ms template window and a 2-s sampling window. The principal component analysis tool was used to analyze the distributions of waveforms comprising each template. In visual cortex at these ages, based on waveform-amplitude differences, no more than two waveforms could be distinguished on one electrode site. Waveforms $>$ 3.5 standard deviations outside each distribution were not included; these waveform outliers were rare and often represented movement artifact or noise ($<$ 1% of all waveforms). After spikes from MUA records were sorted into single units, they were converted to events and a cross-correlation analysis was performed among units obtained from adjacent electrode sites to test for refractory period violations (cutoff = \pm 1 ms). Only nonoverlapping single units were included in these analyses.

Light-evoked neural activity. For each individual unit, perievent histograms (3-s windows, 50-ms bins) were generated with light onset as the trigger. To test for statistical significance, we jittered the timing of light stimulation 1,000 times within a 3-s window with PatternJitter (Amarasingham et al. 2012; Harrison and Geman 2009) implemented in MATLAB (MathWorks, Natick, MA). We generated upper and lower confidence bands ($P <$ 0.05) for each perievent histogram (Amarasingham et al. 2012). Within each age, those units that exhib-

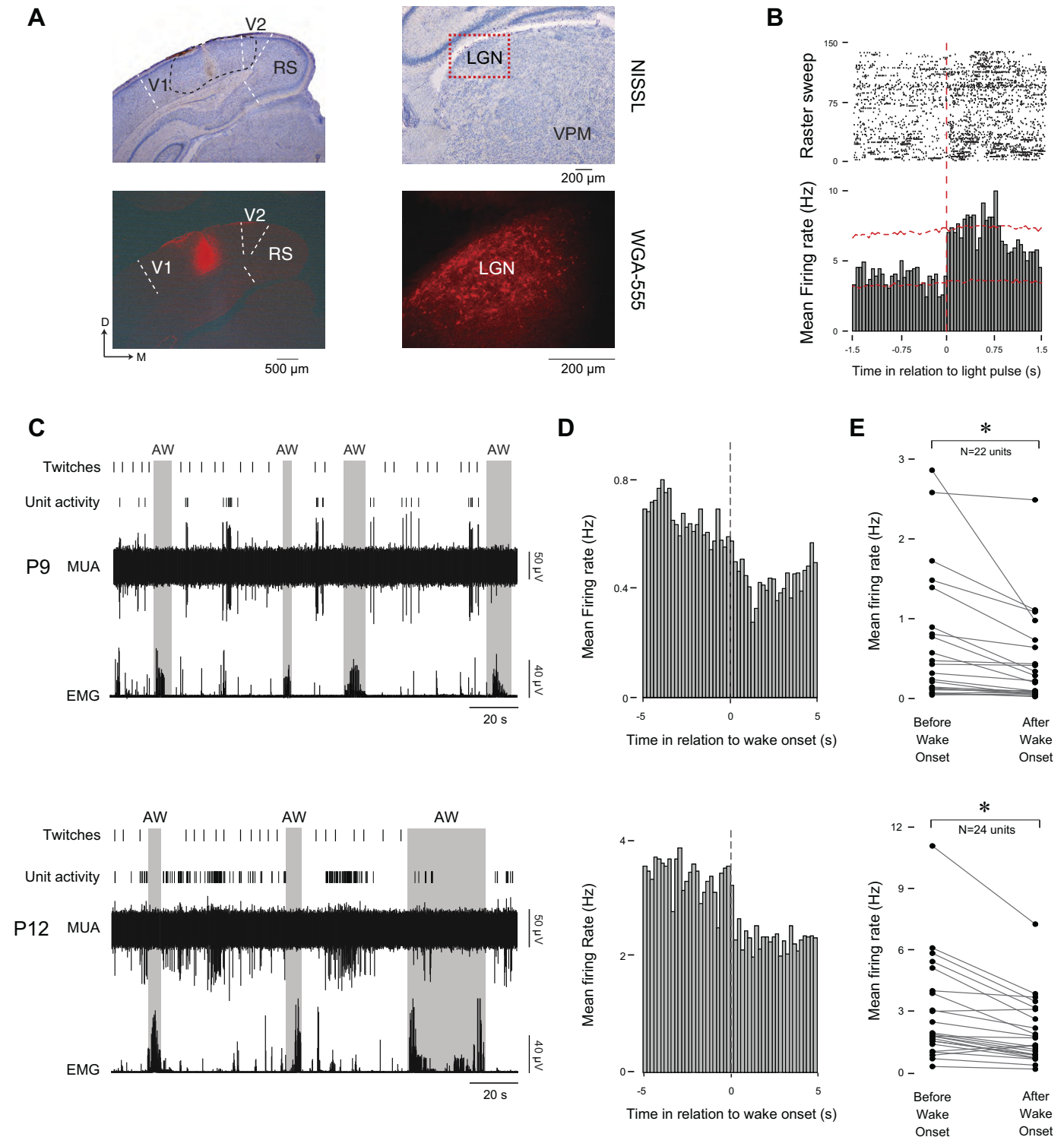


Fig. 1. Visual cortical activity in P9 and P12 rats. *A, top left*: coronal section through occipital cortex in a P9 subject ($\times 2.5$). Black dashed line circumscribes the range of recording sites in primary (V1) and secondary (V2) visual cortex; the sites were similarly distributed at both ages. RS, retrosplenial cortex. *Bottom left*: diffusion of WGA-555 in V1. *Top right*: section stained with cresyl violet ($\times 5$) showing retrograde labeling in the lateral geniculate nucleus (LGN). Dotted red box denotes the labeled area shown in *bottom right* image. VPM, ventral posteromedial thalamic nucleus. *Bottom right*: fluorescent image showing retrograde labeling in the LGN ($\times 20$). At P9 ($n = 2$) and P12 ($n = 2$), retrograde labeling was predominantly restricted to the LGN. D, dorsal; M, medial. *B*: raster plot (*top*) and perievent histogram (*bottom*; 50-ms bins) showing light-evoked activity of cortical units in P12 subjects. Data are pooled across the 6 units (of 24) that exhibited significant light responsiveness. Vertical dashed line denotes onset of light stimulation. Horizontal dashed red lines denote upper and lower confidence bands ($P < 0.05$). *C*: representative recordings of rectified nuchal EMG activity, MUA, and single-unit activity in visual cortex during spontaneous sleep-wake cycling at P9 (*top*) and P12 (*bottom*). Behaviorally scored twitches are shown (vertical ticks). Shaded areas denote periods of active wakefulness (AW). *D*: perievent histograms (200-ms bins) showing mean firing rates of units in relation to wake onset (P9: 22 units, 1,426 AW onsets; P12: 24 units, 732 AW onsets). *E*: line plots showing, for each unit, mean firing rate before and after spontaneous wake onset. $*P < 0.001$.

ited significant increases to light (P9: $n = 2$ units from 2 pups; P12: $n = 6$ units from 6 pups) were pooled together and the jitter analysis was performed again.

Identification of behavioral states. EMG activity and behavioral scoring were used to identify behavioral states (Blumberg et al. 2015). To establish an EMG threshold for distinguishing sleep from wake, EMG signals were rectified and smoothed ($\tau = 0.001$ s). The mean amplitude of high muscle tone and atonia was calculated from five representative 1-s segments, and the midpoint between the two was used to establish the threshold for defining periods of wake (defined as muscle tone being above the threshold for at least 1 s) and sleep (defined as muscle tone being below the threshold for at least 1 s). Active wake (AW) was identified by high-amplitude limb movements (e.g., stepping, stretching) against a background of high muscle tone and was confirmed with behavioral scoring. Active sleep was characterized by the presence of myoclonic twitches of the limbs against a background of muscle atonia. Twitches were identified as sharp EMG events that exceeded by $\geq 3\times$ the mean EMG baseline during atonia; twitches were also confirmed by behavioral scoring (Seelke and Blumberg 2008).

Neural activity at AW onset. For each unit, we identified AW onsets for which there were no other AW onsets within a 5-s window. The records were concatenated across units within age, and perievent histograms (10-s windows, 200-ms time bins) were created with unit activity triggered on AW onsets. In addition, within each unit mean firing rates in 5-s time bins before and after AW onsets were calculated and across units differences were tested with the Wilcoxon matched-pairs signed-rank test.

Rhythmicity. For each sorted unit, we calculated the rhythmicity index (RI), which measures the strength of rhythmicity within a given temporal window, using a previously published method (Arancillo et al. 2015; Sokoloff et al. 2015a). Units with $RI \geq 0.01$ were considered rhythmic. We tested age-related differences in RI and interburst interval with the Mann-Whitney U -test.

Effect of intraocular TTX injection. Firing rates of rhythmic and nonrhythmic units and RIs of rhythmic units, before and after TTX injection, were tested with the Wilcoxon matched-pairs signed-rank test (units with $RI = 0$ were defined as nonrhythmic).

Bursts of cortical activity. When units were categorized as rhythmic, retinal wave-related bursts were identified. To do this, the mean firing frequency of a sorted unit was calculated with an 8-s moving time window. Next, a threshold was determined as 50% of the maximum height of the mean firing frequency for that unit. Only when the firing frequency exceeded the threshold was it identified as a burst.

Effect of spontaneous AW onsets within a burst on unit activity. For each rhythmic unit (P9: 16 units from 7 pups; P12: 14 units from 7 pups), we marked those AW onsets that happened to occur within a burst. (The occurrence of AW onsets within bursts was variable across pups, from 0 to 21 over the 30-min recording sessions; to be included in this analysis, we required at least 4 such events per pup, which yielded 8 units from 4 pups at P9 and 9 units from 6 pups at P12.) The records were concatenated across pups within age, and perievent histograms (4-s windows, 80-ms time bins) were created with unit activity triggered on intraburst AW onset. Finally, within each unit mean firing rates in 2-s time bins before and after AW onsets were

calculated and across units differences were tested with the Wilcoxon matched-pairs signed-rank test.

Effect of evoked AW onsets within a burst on unit activity. In the additional six pups tested at P12 in which the experimenter evoked arousal within a burst, we only included those Stim and No Stim trials in which mean firing frequency exceeded an established threshold. For Stim trials, the latency between trial onset and AW onset (based on EMG activity) was ~ 500 ms. We used this latency to mark the onset of the No Stim trials as well as those Stim trials in which the pup did not wake up. Although the goal of this experiment was to arouse the pup in Stim trials and have the pup sleep through the No Stim trials, a small percentage of Stim trials (6–18%) failed to produce an active wake movement and in a small percentage of No Stim trials (0–21%) the pup exhibited a spontaneous wake movement within the burst. Those trials were included in this analysis. Finally, for each of the six pups, mean unit firing rates in 2-s bins were calculated for each unit before and after the onsets of the Stim and No Stim trials. Values exceeding 2 standard deviations were excluded as outliers for each of the six pups (such outliers occurred only 8 times across all Stim and No Stim trials). Within each individual unit, the mean percent change in firing rate in the Stim and No Stim groups was compared with the Mann-Whitney U -test. We tested the mean percent change across all six units in the Stim and No Stim groups with a paired t -test; we also calculated the effect size for this test (Cohen 1988).

Unless otherwise indicated, α was set at 0.05 for all tests.

RESULTS

We recorded MUA in layers 3–5 of visual cortex at P9 ($n = 9$ pups, 22 units) and P12 ($n = 12$ pups, 24 units) as pups cycled spontaneously between sleep and wake (recordings from all 3 layers were included in these analyses). These two ages roughly correspond to stage II and III retinal waves (Colonnese and Khazipov 2010; Maccione et al. 2014). At both ages across all electrode sites, we identified a mean of two units per pup (range: 1–4 units/pup at P9; 1–6 units/pup at P12; at each age, 3 pups contributed >2 units). At both ages, the majority of electrode sites were within primary visual cortex (V1) and the rest were in secondary visual cortex (V2; Fig. 1A; Table 1). Recordings from both V1 and V2 were included in the analyses (Table 1). As further evidence that the recording sites were within visual cortex, we found that retrograde labeling from this area of cortex was largely restricted to the LGN (Fig. 1A); in addition, although light responsiveness is still developing at these ages, we identified a small proportion of neurons in this area that were activated by light (Fig. 1B; Table 1). Whether light responsive or not, all units were included in these analyses.

At P9 and P12, unit activity was largely expressed as discontinuous bursts against a background of sparse activity (Fig. 1C). The median firing rate was significantly higher at P12 than at P9 (P9: 0.35 Hz, P12: 1.7 Hz; $U = 89$, $P < 0.0001$). At both ages, these bursts appeared to be largely

Table 1. Comparisons of rhythmicity, light responsiveness, and firing rate between units in primary and secondary visual cortex in rats at P9 and P12

Age	Recording Site	No. of Pups	No. of Units	Rhythmic	Light Responsive	Median Firing Rate, Hz
P9	V1	6	15	12/15	2/15	0.46
	V2	3	7	4/7	0/7	0.18
P12	V1	8	19	12/19	5/19	1.97
	V2	4	5	2/5	1/5	1.66

V1, primary visual cortex; V2, secondary visual cortex.

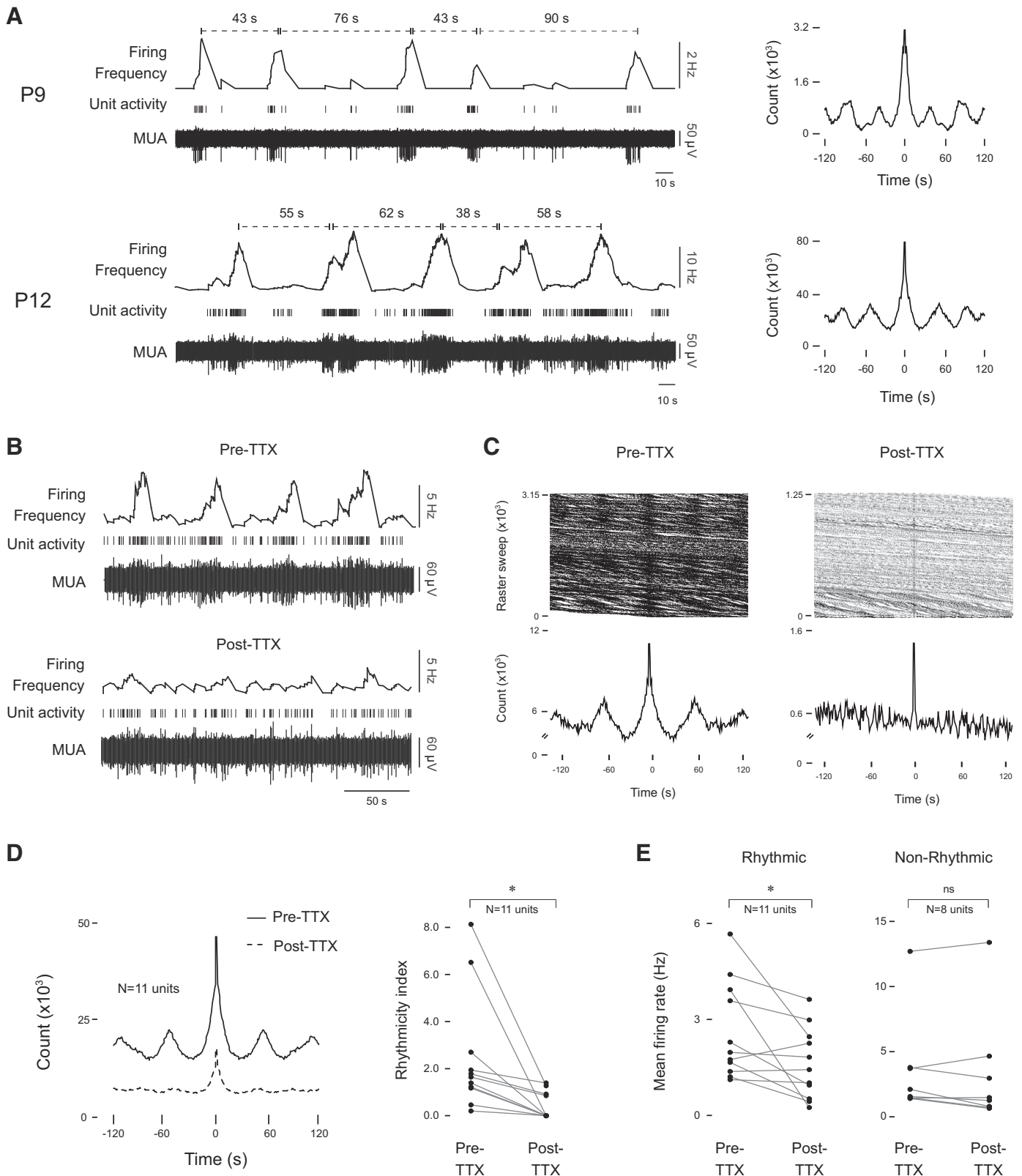


Fig. 2. Rhythmic visual cortical activity is driven by the retina. *A, left*: representative recordings of multiunit activity (MUA), single-unit activity, and mean firing frequency (time window = 8 s) in visual cortex at P9 (*top*) and P12 (*bottom*). Approximate interburst intervals are indicated. *Right*: autocorrelograms showing rhythmic unit activity for the same P9 and P12 subjects. *B*: representative MUA, single-unit activity, and mean firing frequency of a rhythmic unit before (*top*) and after (*bottom*) bilateral intraocular TTX injections. *C*: representative autocorrelograms and raster plots of the same unit shown in *B* before and after TTX. *D*: mean autocorrelogram (*left*) and line plots showing rhythmicity index (*right*) of rhythmic cortical units before and after TTX at P12. $*P < 0.002$. *E*: line plots showing mean firing rate for each rhythmic and nonrhythmic cortical unit before and after TTX. $*P < 0.02$. ns, Not significant.

restricted to periods of sleep and truncated at the onset of AW. To examine this further, we pooled the data at each age and created perievent histograms of firing rate triggered on AW onsets (P9: 1,426 AW onsets, P12: 732 AW onsets; Fig. 1D). The reduction in unit firing rate at AW onset was clear at both ages. Comparison of mean firing rates before and after AW onset revealed significant reductions at both ages (both $P < 0.001$; Fig. 1E). Importantly, because we found no relationship between cortical activity and active sleep-related myoclonic twitches (data not shown), the suppression of activity observed here is not a general response to movement but rather is specific to wake-related movement. Nor did we find any evidence of altered cortical activity at the onset of twitching, which demarcates the boundary between quiet and active sleep (data not shown) (Seelke and Blumberg 2008).

The majority of cortical units at both ages (P9: 16/22 units from 7 pups; P12: 14/24 units from 7 pups) occurred in rhythmic bursts every 30–60 s (Fig. 2A; Table 1). Although the cortical bursts were similarly rhythmic at P9 and P12 (median RI: P9 = 1.01, P12 = 1.52; $U = 85$, $P > 0.2$), the interburst interval of the rhythmic activity at P9 was significantly smaller (medians: P9 = 34.5 s, P12 = 53 s; $U = 9.5$, $P < 0.001$) and the intervals were more variable (median coefficient of variation: P9 = 55.67%, P12 = 45.28%;

$U = 53$, $P < 0.02$). To show that rhythmicity was driven by retinal input, we injected TTX into both eyes in the P12 subjects ($n = 12$ pups, 24 units) and continued recording. In 3 of 12 pups, a total of 5 units were lost during the injection procedure, thus leaving 19 units from 9 pups for analysis. Eleven of these 19 units were rhythmic, and the remaining 8 units were nonrhythmic. TTX significantly decreased rhythmicity in the 11 rhythmic units ($P < 0.002$, Fig. 2, B–D). In addition, TTX significantly decreased the mean firing rates of the rhythmic units ($P < 0.02$) but had no significant effect on the nonrhythmic units ($P > 0.2$; Fig. 2E). The timing and TTX sensitivity of the rhythmic bursts of cortical activity mirror those of retinal waves, which also occur every 30–60 s (Ackman et al. 2012; Colonnese and Khazipov 2010; Hanganu et al. 2006) and are blocked by intraocular injections of TTX (Hanganu et al. 2006).

The suggestion that wake onset suppresses visual cortical activity would be strengthened by evidence of wake-related suppression within a burst. To provide such evidence, we examined rhythmic units and identified wake onsets that occurred spontaneously within a burst (P9: $n = 62$ AW onsets across 8 units and 4 pups; P12: $n = 103$ AW onsets across 9 units and 5 pups). The small sample sizes reflect the use of a strict criterion to identify AW onsets within bursts, as well as

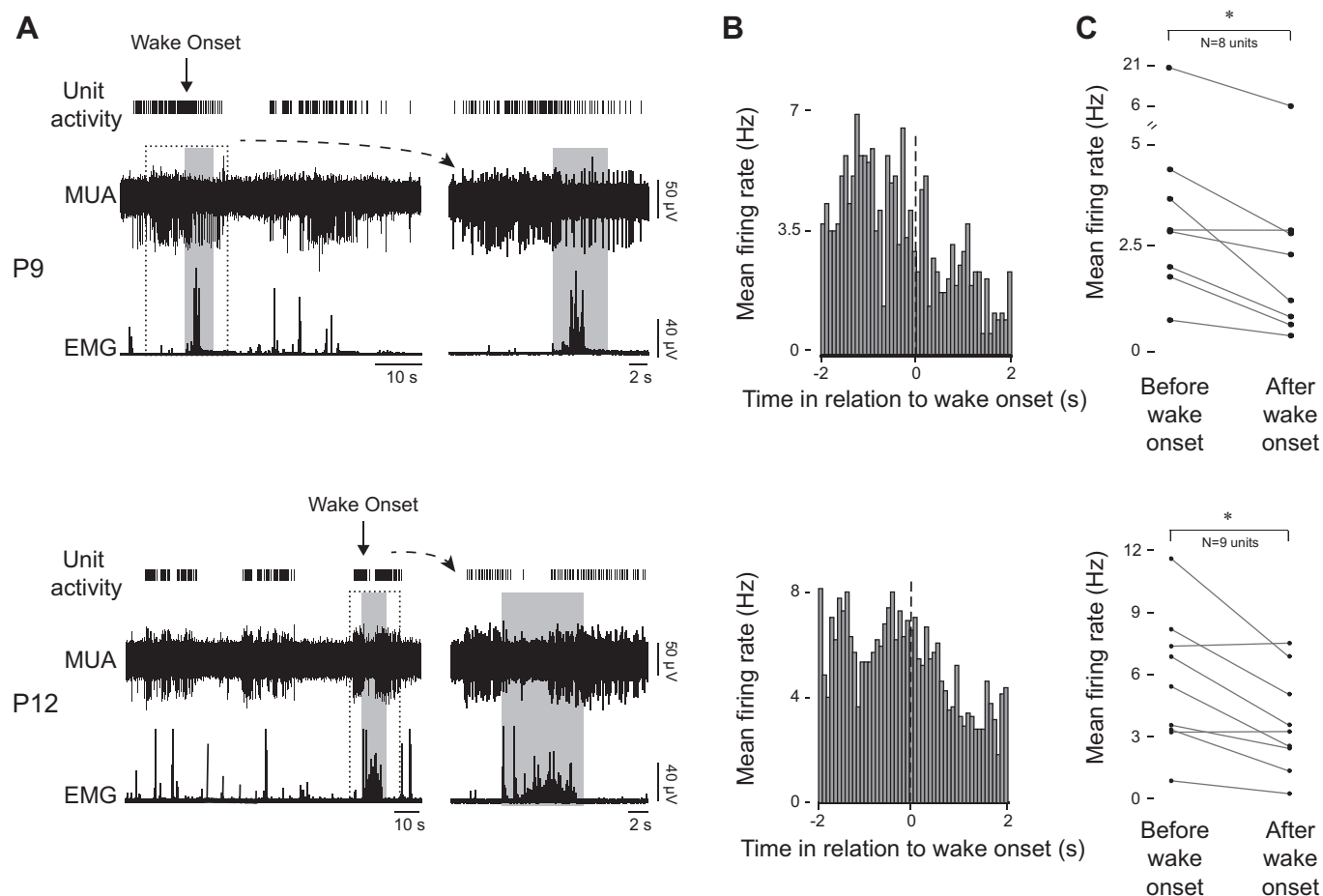


Fig. 3. Spontaneous wake onset suppresses rhythmic visual cortical activity at P9 (top) and P12 (bottom). *A*: representative recordings of rectified nuchal EMG activity, multiunit activity (MUA), and single-unit activity during periods when spontaneous wake onsets occurred within a retinal wave-related burst. Two different timescales are shown; dashed boxes in the left-hand recordings define the region of the right-hand recordings. Shaded gray bars denote active wake periods. *B*: perievent histograms (80-ms bins) of mean firing rates of rhythmic cortical units when wake onset occurred within a burst (P9: 8 units, 62 AW onsets; P12: 9 units, 103 AW onsets). *C*: line plots showing mean firing rate for each rhythmic unit before and after spontaneous wake onsets within a burst. $*P < 0.03$.

the low probability that such events occurred over the 30-min recording sessions. Nonetheless, the available data suggest that spontaneous awakenings truncate cortical bursts. Representative recordings at P9 and P12 illustrate the coincidence of AW onset with intraburst decreases in unit activity (Fig. 3A). Perievent histograms of pooled data show intraburst decreases in firing rate at AW onset at both ages (Fig. 3B). When mean unit firing rates before and after AW onset were compared, there was a significant reduction at both ages (both $P < 0.03$; Fig. 3C).

Finally, to provide stronger, causal evidence for wake-related suppression of visual cortical activity, we tested an additional six subjects at P12 (1 rhythmic unit per pup) in which active wake movements were or were not evoked by an experimenter (Stim and No Stim groups, respectively). Stimulation was effective at evoking arousal in 82–94% of all Stim trials; in addition, pups did not exhibit spontaneous wakefulness in 79–100% of No Stim trials. The representative recordings in Fig. 4A show a substantial intraburst decrease in unit activity after evoked AW onset during a Stim trial; a representative recording for a No Stim trial is also shown. Within each of the six individual units, the mean percent decrease in firing rates was significantly greater in the Stim group than in the No Stim group (range of U values: 52.5–244.5, all $P < 0.04$; Fig. 4B, left). Averaging across the six units, the mean percent decrease was also significantly greater in the Stim group ($t = 5.47$, $df = 5$, $P < 0.003$; Cohen's $d = 3.44$; Fig. 4B, right).

DISCUSSION

We show here in the visual cortex of infant rats that spontaneous unit activity, like local field activity (Colonnese and Khazipov 2010; Hanganu et al. 2006; Murata and Colonnese 2016), occurs in rhythmic bursts. We found that these rhythmic bursts are suppressed by the onset of active wake movements—whether those movements occur spontaneously or are evoked by an experimenter.

A role for sleep has been implicated in developmental plasticity in a variety of systems. For example, in the visual system sleep deprivation prevents induction of long-term potentiation in visual cortex in postweanling rats and delays the normal course of cortical maturation (Shaffery et al. 2002). Sleep deprivation also affects remodeling of cortical ocular dominance columns in kittens (Frank et al. 2001). In contrast, retinal waves are present much earlier in development and have been implicated in visual cortical plasticity (Huberman et al. 2006). In finding that wake onset suppresses activity in visual cortex at ages when retinal waves provide the predominant input, these results suggest a permissive role for sleep in visual cortical plasticity at earlier ages than has been previously considered (Frank et al. 2001; Shaffery et al. 2002).

The suppression of visual cortical activity during wake at these ages cannot persist when, only a few days later, the eyes open, retinal waves cease, spontaneous cortical activity is continuous, and visually guided behavior begins. Nonetheless, visual cortical activity continues to be modulated by behavioral state but in a different form. Specifically, immediately after eye opening in mice, visual cortical activity increases at the transition from immobility to running (Hoy and Niell 2015); this modulatory effect of behavioral state continues into adulthood

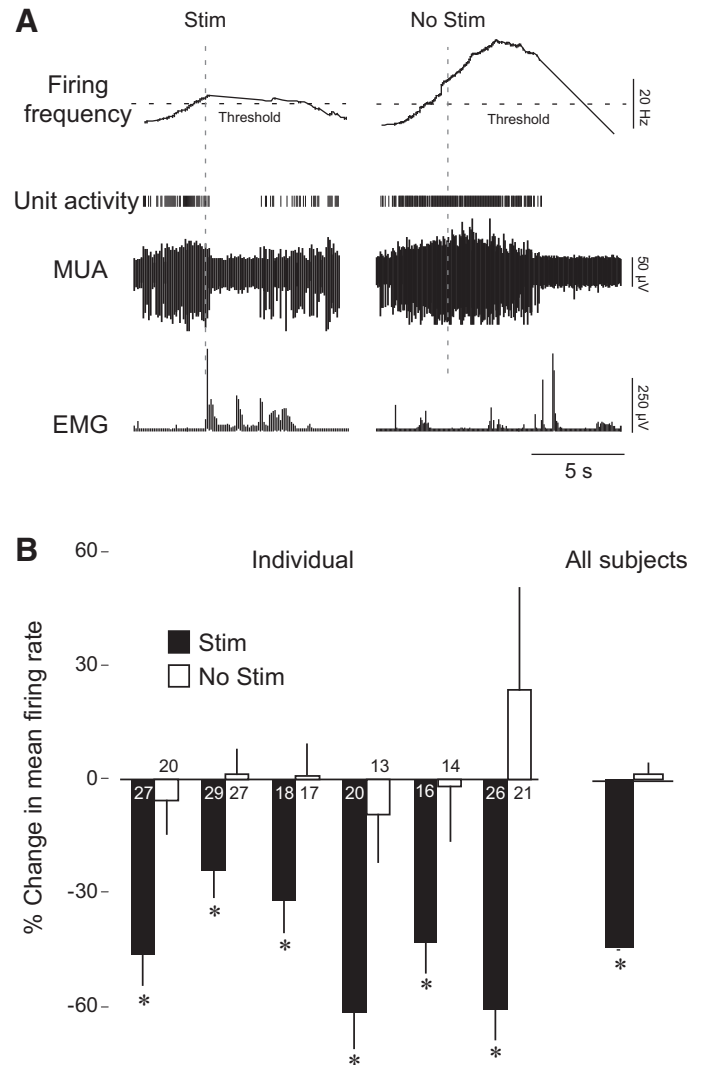


Fig. 4. Experimentally evoked active wake onset suppresses rhythmic visual cortical activity. *A*: representative recording of rectified nuchal EMG activity, multiunit activity (MUA), single-unit activity, and mean firing frequency (time window = 8 s) in a P12 subject during a Stim (*left*) and a No Stim (*right*) trial. Vertical dashed lines denote trial onset. Horizontal dashed lines denote the threshold for defining a retinal wave-related burst. *B*, *left*: bar graphs showing mean % changes in firing rates across all Stim and No Stim trials for each individual subject. Changes were computed based on mean (\pm SE) firing rates in the 2-s periods before and after trial onset. Numbers of Stim and No Stim trials are indicated for each pup. * $P < 0.04$. *Right*: mean (\pm SE) % change in firing rate for the Stim and No Stim groups. $n = 6$ units per group. * $P < 0.003$.

(Niell and Stryker 2010). In the context of the present results, such findings suggest that complex interactions between behavioral state and visual system processing are expressed throughout the life span but that these interactions are expressed in very different ways depending upon the functional requirements of the system.

The present findings parallel those in the sensorimotor system in that spontaneous activity arising from peripheral structures (i.e., retina, limbs) preferentially activates neural circuits during sleep (Blumberg et al. 2013). This parallel may reflect a general principle of sensory system development and could help to explain why sleep is so abundant in early development across a diversity of species (Kayser and Biron 2016).

ACKNOWLEDGMENTS

We thank Jimmy Dooley, Carlos Del Rio-Bermudez, and Alex Tiriac for helpful comments.

GRANTS

This research was supported by National Institute of Child Health and Human Development Grants R37 HD-081168 and R01 HD-063071 to M. S. Blumberg.

DISCLOSURES

No conflicts of interest, financial or otherwise, are declared by the authors.

AUTHOR CONTRIBUTIONS

D.M. and M.S.B. conceived and designed research; D.M. and A.J.Y. performed experiments; D.M., A.J.Y., and G.S. analyzed data; D.M. and M.S.B. interpreted results of experiments; D.M., A.J.Y., and M.S.B. prepared figures; D.M. and M.S.B. drafted manuscript; D.M., G.S., and M.S.B. edited and revised manuscript; D.M., G.S., and M.S.B. approved final version of manuscript.

REFERENCES

- Ackman JB, Burbridge TJ, Crair MC. Retinal waves coordinate patterned activity throughout the developing visual system. *Nature* 490: 219–225, 2012. doi:10.1038/nature11529.
- Adelsberger H, Garaschuk O, Konnerth A. Cortical calcium waves in resting newborn mice. *Nat Neurosci* 8: 988–990, 2005. doi:10.1038/nn1502.
- Amarasingham A, Harrison MT, Hatsopoulos NG, Geman S. Conditional modeling and the jitter method of spike resampling. *J Neurophysiol* 107: 517–531, 2012. doi:10.1152/jn.00633.2011.
- Arancillo M, White JJ, Lin T, Stay TL, Sillitoe RV. In vivo analysis of Purkinje cell firing properties during postnatal mouse development. *J Neurophysiol* 113: 578–591, 2015. doi:10.1152/jn.00586.2014.
- Blankenship AG, Feller MB. Mechanisms underlying spontaneous patterned activity in developing neural circuits. *Nat Rev Neurosci* 11: 18–29, 2010. doi:10.1038/nrn2759.
- Blumberg MS, Marques HG, Iida F. Twitching in sensorimotor development from sleeping rats to robots. *Curr Biol* 23: R532–R537, 2013. doi:10.1016/j.cub.2013.04.075.
- Blumberg MS, Sokoloff G, Tiriac A, Del Rio-Bermudez C. A valuable and promising method for recording brain activity in behaving newborn rodents. *Dev Psychobiol* 57: 506–517, 2015. doi:10.1002/dev.21305.
- Butts DA, Kanold PO, Shatz CJ. A burst-based “Hebbian” learning rule at retinogeniculate synapses links retinal waves to activity-dependent refinement. *PLoS Biol* 5: e61, 2007. doi:10.1371/journal.pbio.0050061.
- Cohen J. *Statistical Power Analysis for the Behavioral Sciences*. Hillsdale, NJ: Erlbaum, 1988.
- Colonnese MT, Kaminska A, Minlebaev M, Milh M, Bloem B, Lescure S, Moriette G, Chiron C, Ben-Ari Y, Khazipov R. A conserved switch in sensory processing prepares developing neocortex for vision. *Neuron* 67: 480–498, 2010. doi:10.1016/j.neuron.2010.07.015.
- Colonnese MT, Khazipov R. “Slow activity transients” in infant rat visual cortex: a spreading synchronous oscillation patterned by retinal waves. *J Neurosci* 30: 4325–4337, 2010. doi:10.1523/JNEUROSCI.4995-09.2010.
- Frank MG, Issa NP, Stryker MP. Sleep enhances plasticity in the developing visual cortex. *Neuron* 30: 275–287, 2001. doi:10.1016/S0896-6273(01)00279-3.
- Gramsbergen A, Schwartze P, Precht HF. The postnatal development of behavioral states in the rat. *Dev Psychobiol* 3: 267–280, 1970. doi:10.1002/dev.420030407.
- Hanganu IL, Ben-Ari Y, Khazipov R. Retinal waves trigger spindle bursts in the neonatal rat visual cortex. *J Neurosci* 26: 6728–6736, 2006. doi:10.1523/JNEUROSCI.0752-06.2006.
- Harrison MT, Geman S. A rate and history-preserving resampling algorithm for neural spike trains. *Neural Comput* 21: 1244–1258, 2009. doi:10.1162/neco.2008.03-08-730.
- Hoy JL, Niell CM. Layer-specific refinement of visual cortex function after eye opening in the awake mouse. *J Neurosci* 35: 3370–3383, 2015. doi:10.1523/JNEUROSCI.3174-14.2015.
- Huberman AD, Feller MB, Chapman B. Mechanisms underlying development of visual maps and receptive fields. *Annu Rev Neurosci* 31: 479–509, 2008. doi:10.1146/annurev.neuro.31.060407.125533.
- Huberman AD, Speer CM, Chapman B. Spontaneous retinal activity mediates development of ocular dominance columns and binocular receptive fields in V1. *Neuron* 52: 247–254, 2006. doi:10.1016/j.neuron.2006.07.028.
- Jouvet-Mounier D, Astic L, Lacote D. Ontogenesis of the states of sleep in rat, cat, and guinea pig during the first postnatal month. *Dev Psychobiol* 2: 216–239, 1970. doi:10.1002/dev.420020407.
- Karlsson KA, Gall AJ, Mohs EJ, Seelke AM, Blumberg MS. The neural substrates of infant sleep in rats. *PLoS Biol* 3: e143, 2005. doi:10.1371/journal.pbio.0030143.
- Katz LC, Shatz CJ. Synaptic activity and the construction of cortical circuits. *Science* 274: 1133–1138, 1996. doi:10.1126/science.274.5290.1133.
- Kayser MS, Biron D. Sleep and development in genetically tractable model organisms. *Genetics* 203: 21–33, 2016. doi:10.1534/genetics.116.189589.
- Kilb W, Kirischuk S, Luhmann HJ. Electrical activity patterns and the functional maturation of the neocortex. *Eur J Neurosci* 34: 1677–1686, 2011. doi:10.1111/j.1460-9568.2011.07878.x.
- Maccione A, Hennig MH, Gandolfo M, Muthmann O, van Coppenhagen J, Eglen SJ, Berdondini L, Sernagor E. Following the ontogeny of retinal waves: pan-retinal recordings of population dynamics in the neonatal mouse. *J Physiol* 592: 1545–1563, 2014. doi:10.1113/jphysiol.2013.262840.
- Marder E, Rehm KJ. Development of central pattern generating circuits. *Curr Opin Neurobiol* 15: 86–93, 2005. doi:10.1016/j.conb.2005.01.011.
- Mirmiran M, Corner M. Neuronal discharge patterns in the occipital cortex of developing rats during active and quiet sleep. *Brain Res* 255: 37–48, 1982. doi:10.1016/0165-3806(82)90074-8.
- Mooney R, Penn AA, Gallego R, Shatz CJ. Thalamic relay of spontaneous retinal activity prior to vision. *Neuron* 17: 863–874, 1996. doi:10.1016/S0896-6273(00)80218-4.
- Murata Y, Colonnese MT. An excitatory cortical feedback loop gates retinal wave transmission in rodent thalamus. *eLife* 5: e18816, 2016. doi:10.7554/eLife.18816.
- Niell CM, Stryker MP. Modulation of visual responses by behavioral state in mouse visual cortex. *Neuron* 65: 472–479, 2010. doi:10.1016/j.neuron.2010.01.033.
- Seelke AM, Blumberg MS. The microstructure of active and quiet sleep as cortical delta activity emerges in infant rats. *Sleep* 31: 691–699, 2008. doi:10.1093/sleep/31.5.691.
- Shaffery JP, Sinton CM, Bisette G, Roffwarg HP, Marks GA. Rapid eye movement sleep deprivation modifies expression of long-term potentiation in visual cortex of immature rats. *Neuroscience* 110: 431–443, 2002. doi:10.1016/S0306-4522(01)00589-9.
- Sokoloff G, Plumeau AM, Mukherjee D, Blumberg MS. Twitch-related and rhythmic activation of the developing cerebellar cortex. *J Neurophysiol* 114: 1746–1756, 2015a. doi:10.1152/jn.00284.2015.
- Sokoloff G, Uitermarkt BD, Blumberg MS. REM sleep twitches rouse nascent cerebellar circuits: implications for sensorimotor development. *Dev Neurobiol* 75: 1140–1153, 2015b. doi:10.1002/dneu.22177.
- Wong RO. Retinal waves and visual system development. *Annu Rev Neurosci* 22: 29–47, 1999. doi:10.1146/annurev.neuro.22.1.29.